Acta Neuropathol_ (2006) 112: 205–215
DOI 10.1007/s00401-006-0082-8

ORIGINAL PAPER

Annett Hölsken · Ilker Y. Eyüpoglu · Mike Lueders
Christian Tränkle · Detlef Dieckmann · Rolf Buslei
Eric Hahnen · Ingmar Blümcke · Florian A. Siebzehnrübl

Ex vivo therapy of malignant melanomas transplanted into organotypic brain slice cultures using inhibitors of histone deacetylases

Received: 4 November 2005 / Revised: 28 April 2006 / Accepted: 28 April 2006 / Published online: 14 June 2006

Abstract Disease progression in patients suffering from malignant melanomas is often determined by metastatic spreading into brain parenchyma. Systemic chemotherapy regimens are, therefore, mandatory for successful treatment. Most recently, inhibitors of histone deacetylases (HDACi) have been shown to significantly inhibit melanoma progression. Here, mouse as well as human melanoma cells were transplanted into rodent hippocampal slice cultures in order to translate and microscopically confirm promising in vitro chemotherapeutic propensities of HDACi within the organotypic brain environment. In our ex vivo model, tumor progression was significantly inhibited by administration of low micromolar concentrations of second generation HDACi MS-275 over a period of 8 days. In contrast, HDACi treatment with suberoylanilide hydroxamic acid was less efficient ex vivo, although both compounds were successful in the treatment of tumor cell monolayer cultures. Protein levels of the cell cycle inhibitor $p21^{WAF1}$ were significantly increased after HDACi treatment, which points to enhanced G1 arrest of tumor cells as confirmed by cytofluorometric analysis. Considering the ability of MS-275 to cross the blood–brain barrier, our experimental model identifies the benzamide MS-275 as a promising therapeutic compound for targeting epigenetic chromatin modulation as systemic treatment of metastatic melanomas.

Keywords MS-275 · Valproic acid · SAHA · M344 · Hippocampus · p21 · Melanoma metastases

A. Hölsken · R. Buslei · E. Hahnen · I. Blümcke (✉)
F. A. Siebzehnrübl
Department of Neuropathology,
University of Erlangen-Nuremberg,
Krankenhausstr. 8-10, 91054 Erlangen, Germany
E-mail: bluemcke@neuropatho.med.uni-erlangen.de
Tel.: +49-9131-8526031
Fax: +49-9131-8526033

I. Y. Eyüpoglu
Department of Neurosurgery,
University of Erlangen-Nuremberg, Erlangen, Germany

M. Lueders
Department of Medicine I,
University of Erlangen-Nuremberg, Erlangen, Germany

C. Tränkle
Department of Pharmacology and Toxicology,
Institute of Pharmacy, University of Bonn, Bonn, Germany

D. Dieckmann
Department of Dermatology,
University of Erlangen-Nuremberg, Erlangen, Germany

E. Hahnen
Institute of Human Genetics, Institute of Genetics and
Center for Molecular Medicine Cologne (CMMC),
University of Cologne, Cologne, Germany

Introduction

Malignant melanomas are amongst the most prevalent cancers worldwide [47, 18]. Mortality risk is determined by systemic metastasis most commonly into the lung, liver and brain [12, 36]. Spreading of melanomas into the brain is clinically observed in 10–40% of patients, but autopsy studies suggest that these numbers are underestimated [2]. Since neurosurgical resection of multiple melanoma metastases within the CNS cannot be successfully achieved, adjuvant chemo- or radiotherapy is warranted [2, 20, 40]. Current treatment modalities include a combination of the alkylating agent temozolomide and whole-brain radiotherapy [1] or systemic fotemustine administration [26]. However, metastatic melanomas are often characterized by multidrug resistance [19] and only a small proportion of patients survive more than 2 years after metastasis becomes evident [12].

Recent data point to the efficacy of histone deacetylase (HDAC) inhibitors as promising chemotherapeutic drugs for malignant melanomas [5, 11, 50]. Epigenetic

regulation of chromatin structure by HDAC inhibitors induces deregulation of approximately 2–10% of gene expression in eucaryotic cells, but is largely dependent on subjected cell types [15, 30]. Core histone acetylation at distinct lysine residues is associated with transcriptional activation, whereas deacetylation followed by methylation induces gene silencing [13, 24]. Acetylation of core histones is mediated by histone acetyltransferase activity and represents a short-term physiological mechanism crucially involved in many processes during development and aging. The therapeutic propensity of HDAC inhibitors in cancer and neurological diseases has, however, been recently established [4, 21, 41] and is already confirmed in several clinical trials [34, 48]. Various pharmacological substances have been identified as selective HDAC inhibitors, amongst which the second generation compounds suberoylanilide hydroxamic acid (SAHA), as well as MS-275 and M344 are most promising [25, 31, 33, 39]. However, the benzamide (MS-275) and hydroxamate (SAHA) classes of HDAC inhibitors exhibit different specificities for HDAC isoforms. MS-275 interacts primarily with HDAC class I [34]. Even within class I HDACs, MS-275 acts differently onto specific HDAC isoforms [22, 39]. Therefore, HDAC inhibitory actions appear to be dependent on cell types and brain regions [44].

Experimental paradigms remain a challenge to systematically study anti-cancer effects as well as clinical side effects within the central nervous system, i.e., neurotoxicity of novel chemotherapeutic drugs. The recently established hippocampal slice culture model for tumor progression is, therefore, helpful in many respects [10]. On the other hand, ex vivo brain slices lack blood supply, perfusion and a blood–brain barrier. In addition, structural and molecular reorganization may compromise hippocampal networks [10]. However, cellular as well as pharmacological interactions between grafted tumor cells and the organotypic brain environment can be successfully analyzed for up to 3 weeks and are in this period accessible for continuous experimental treatment and monitoring [10]. Although this approach needs to be confirmed in vivo, organotypic brain slice cultures may bridge the gap between monolayer experiments and in vivo studies [7, 9, 23, 45]. Here, we examined whether anti-tumor action of HDAC inhibitors on melanoma cells in cell culture also applies to tumor growth reduction in a more complex microenvironment resembling cerebral metastases.

Materials and methods

Monolayer cell culture

B16/F10 murine melanoma cells (obtained from ATCC, Manassas, VA, USA) were cultured in modified DMEM medium (Biochrom AG, Berlin, Germany) containing 4 mM L-glutamine (Gibco, Karlsruhe, Germany), 4 g/l glucose (Merck, Darmstadt, Germany), 100 units/ml penicillin, 100 µg/ml streptomycin (Sigma–Aldrich, Schnelldorf, Germany) and 10% FCS (Biochrom AG, Berlin, Germany). All monolayer experiments were performed in a humidified atmosphere at 37°C and 5% CO_2. The B16/F10 cell line has been shown to be highly metastatic in various in vivo models [37], and is therefore specifically qualified for the ex vivo brain metastasis slice culture model. Human melanoma cell lines MM1 and MM2 were obtained from the Department of Dermatology, University Hospital Erlangen, from surgically removed metastasis after patients informed consent was given [38]. Cells were cultured in RPMI containing 10% FCS (BioWhittaker, Walkersville, MD, USA), 20 µg/ml gentamycin (Sigma-Aldrich, Schnelldorf, Germany) and 2 mM glutamine (BioWhittaker, Walkersville, MD, USA). Cells were grown at 37°C in a humidified atmosphere of 5% CO_2.

Chemicals

N-(2-Aminophenyl)-4-[*N*-(pyridine-3-ylmetoxycarbonyl) aminomethyl]benzamide (MS-275) and *N*-hydroxy-7-(4-dimethylaminobenzoyl)aminoheptanamide (M344) were obtained from Calbiochem (Bad Soden, Germany). Valproic acid (VPA) was supplied from Sigma-Aldrich (Schnelldorf, Germany). SAHA was purchased from Alexis Biochemicals (Grünberg, Germany). VPA was dissolved in H_2O. All other compounds were dissolved in DMSO (Sigma-Aldrich, Schnelldorf, Germany) and diluted in medium at specified concentrations prior to experimental use.

Microscopical evaluation

Morphometrical analysis was performed using high power optical fields digitized with a CCD camera (Color View II, Soft Imaging System, Münster, Germany) equipped to a BX51 microscope (Olympus GmbH, Hamburg, Germany) and respective imaging software (analySIS, Soft Imaging System, Münster, Germany). Fluorescence-labeled tumor cells transplanted to organotypic brain slice cultures were analyzed by an Olympus microscope (IX 70) equipped with a fluorescein isothiocyanate narrow band filter (excitation filter 450–490 nm, band filter 520–550), a CCD camera (F-View II, Soft Imaging System, Münster, Germany) and imaging software as above. Statistical significance was calculated with Mann–Whitney *U* test (Statview II, Abacus, Berkeley, CA, USA). The tumor size was calculated as area of transplanted melanoma cells identified either by intracellular melanin content or eGFP labeling (see below), respectively, using analySIS software.

MTT assay

Viable cell numbers were estimated by 3-(4,5-dimethylthiazol-2-yl)-2,5-diphenyl-tetrazolium-bromide (MTT) assay [9, 35]. Briefly, 2,000 melanoma cells/ml were seeded in a 96-well plate (final volume was 250 µl/well). Forty-eight hours after seeding, cells were treated either

with MS-275, SAHA, M344 or VPA. At 96 h incubation, 0.5 mg/ml MTT (Sigma–Aldrich, Schnelldorf, Germany) dissolved in medium was applied for 2 h. Subsequently, the medium was discarded and each well was incubated with 100 µl of an isopropanol stock solution containing 165 µl hydrochloric acid per 50 ml isopropanol. Optical densities of each well were determined using a microplate reader (Tecan, Crailsheim, Germany) set to 550 nm (wavelength correction set to 690 nm).

Data analysis

Concentration–effect curves for the inhibition of cell viability following drug treatment were generated by nonlinear regression analysis using GraphPad Prism version 4.00 for Windows (GraphPad Software, San Diego, CA, USA). Data were fitted to a four parameter logistic equation comprising the top plateau, bottom plateau, inflection point IC_{50} and curve slope n_H. The parameters IC_{50} and n_H were set as variables, "top" was the control value of cell viability and was set constant = 100%. Cell viability approached zero in the presence of high concentrations of the test compounds and extended incubation times. Therefore, the parameter "bottom" was set constant = 0 in the nonlinear regression analyses.

Protein preparation and immunoblotting

Melanoma cells were treated either with MS-275, SAHA or solvent controls. After 24 h cells were pelleted by centrifugation at 175*g* for 10 min and the supernatant fraction was decanted. Cells were washed three times with PBS and suspended in lysis buffer. For histone immunoblotting, lysis buffer contained 10 mM HEPES, pH 7.9; 1.5 mM $MgCl_2$; 10 mM KCl; 0.5 mM DTT; 1.5 mM PMSF. Sulfuric acid was added to a final concentration of 0.2 M. The cells were incubated for 30 min on ice and centrifuged thereafter at 11,000*g* for 10 min at 4°C. The supernatant fraction was dialyzed against 200 ml 0.1 M acetic acid for 2 × 1 h and against 200 ml H_2O thereafter (1 h, 3 h and overnight). The protein preparation for $p21^{WAF1}$ detection comprised cell lysation with lysis buffer containing 50 mM Tris–Buffer pH 8, 150 mM NaCl, 1% Triton-X-100, 1 mM EDTA pH 8, 1.0% SDS, 1 mM PMSF and one tablet of protease inhibitor cocktail (Roche, Mannheim, Germany). The supernatant extraction was prepared as described before, excluding dialysis procedure. Protein concentrations of the supernatant were evaluated by photometric measurement (Tecan, wavelength set to 562 nm) using the BCA Assay kit (Uptima, Montelucon, France). Protein extracts were subjected to SDS-polyacrylamide gel electrophoresis on a 12% polyacrylamide gel. Ten micrograms of the soluble fraction were loaded per lane. Separated proteins were electroblotted onto nitrocellulose membrane (0.2 µm pore size; Schleicher & Schuell, Dassel, Germany). Equal protein loading was estimated using immunostaining with a monoclonal mouse anti-β-actin antibody (1:10,000, Sigma-Aldrich, Schnelldorf, Germany). Controls and treated melanoma cells were analyzed for acetylated histone H3 using polyclonal rabbit anti-acetyl histone H3 (1:450, Biomol, Hamburg, Germany), monoclonal mouse anti-$p21^{WAF1}$ antibody (1:200, Dako, Glostrup, Denmark) and chemiluminescence detection (Amersham, Freiburg, Germany).

Flow cytometry

Melanoma cells were treated after MS-275 and SAHA exposition with an ice-cold hypotonic solution of propidium iodide (Sigma–Aldrich, Schnelldorf, Germany) for 30 min in the dark. Adherent as well as floating cells were included and apoptosis and cell cycle distribution were analyzed using flow cytometry (FACS-Calibur, BD Biosciences, Heidelberg, Germany) and Cell Quest software [27]. Statistical significance was calculated with Mann–Whitney *U* test (Statview II).

eGFP transfection of melanoma cells

Melanoma cells were transfected with pEGFP-N1 (BD Biosciences Clontech, Heidelberg, Germany) using calcium phosphate coprecipitation [43]. Briefly, melanoma cells were cultured in 1.9 cm^2 dishes at a density of 100,000 cells/well in 500 µl culture medium. Twenty-four hours later the medium was discarded and 500 µl of DNA precipitate/well were added to the cells. The DNA precipitate was generated by adding 417.5 µl sterile water, 62.5 µl 2 M $CaCl_2$, 20 µg plasmid DNA, 500 µl BES buffer into a final volume of 10 ml culture medium. The BES buffer contained 1.07 g BES (*N,N* bis-[2-hydroxyethyl]-2-aminoethanesulfonic acid, Sigma-Aldrich, Schnelldorf, Germany), 1.63 g NaCl and 26.7 mg $Na_2HPO_4 \times 2H_2O$ dissolved in 100 ml sterile water at a pH of 6.95.

Cells were incubated at 37°C and 5% CO_2 for 20 h. Precipitate-containing medium was removed and the cells were cultured in primary culture medium for 24 h. The eGFP positive cells were sorted (MoFlo, DakoCytomation) three times to accelerate selection process.

Organotypic hippocampal slice cultures

Slice cultures were prepared and maintained as described [8]. Six-day-old Wistar rats and 7-day-old C57/Bl6 mice were used, respectively. After decapitation, the brains were rapidly removed and placed into ice-cold preparation medium containing Hank's balanced salt solution (Gibco, Karlsruhe, Germany) with 10% normal horse serum (Biochrom, Berlin, Germany). After dissection of the frontal pole of the hemispheres and the cerebellum, the brains were cut in 350 µm thick horizontal slices in preparation medium using a vibratome (Leica VT 1000S, Bensheim, Germany). The slices were transferred into culture plate insert membrane dishes (Becton Dickinson, Heidelberg, Germany; pore size 0.4 µm) and subsequently transferred into six-well culture dishes (Becton Dickinson, Heidelberg, Germany) containing 1.2 ml

culture medium (MEM–HBSS, 2:1, 25% normal horse serum, 2% L-glutamine, 2.64 or 14.3 mg/ml glucose, 100 U/ml penicillin, 0.1 mg/ml streptomycin, 10 µg/ml insulin–transferrin–sodium selenite supplement and 0.8 µg/ml vitamin C), according to the interface technique [46]. The slices were cultured in humidified atmosphere at 35°C and 5% CO_2. The medium was changed 1 day after preparation and every second day thereafter.

Organotypic melanoma invasion model

Five thousand eGFP-positive melanoma cells were implanted within a total volume of 0.05 µl medium into the entorhinal cortex 24 h after slice preparation [10]. One day after implantation and every other day, melanoma growth and invasion were evaluated using an inverse fluorescence microscope (details see above). Experimental ex vivo melanoma treatment was started the day following tumor transplantation or 4 days thereafter, by addition of HDAC inhibitors SAHA and MS-275 to the medium.

Histological examination

Slices were fixed with a solution containing 40 g/l paraformaldehyde dissolved in aqua dest., 15% picric acid, 50% PBS pH 7.3 and 0.1% glutaraldehyde for 15 min. Thereafter, tissue slices were transferred into the same fixative without glutaraldehyde and stored at 4°C over night. After rinsing in PBS, slices were stored at 4°C in 30% sucrose solution for 1 week, then rinsed in PBS. For histological analyses, 12 µm thick horizontal sections of tissue were prepared using a cryomicrotome (Cryo-Star HM560, MICROM, Walldorf, Germany) and hematoxylin–eosin staining.

Immunohistochemical $p21^{WAF1}$ staining was performed using slices containing an established melanoma tumor (4 days after B16/F10 transplantation). Transplanted slices were treated either 24 h with SAHA ($3 \times IC_{90}$) and MS-275 ($1 \times IC_{90}$) or 48 h with MS-275 ($1 \times IC_{90}$). Thereafter, tissue was fixed and sectioned as described above. Slides were incubated for 30 min with monoclonal mouse anti-$p21^{WAF1}$ antibody (1:30, Dako, Glostrup, Denmark) and counterstained with hematoxylin after using the diaminobenzidine (DAB) detection kit (Ventana, Illkirch, France).

Results

MS-275 reduces murine melanoma cell growth in vitro

In a first set of experiments, the propensity of HDAC inhibitors to reduce melanoma cell viability was analyzed in vitro. Mouse B16/F10 cells were incubated with various concentrations of test compounds, i.e., the benzamides MS-275 and M344, SAHA and VPA for 96 h. A sigmoidal relationship between drug concentration and tumor cell viability was observed in all experiments. All compounds completely inhibited cell growth. However, the inhibitory potency differed considerably between the tested drugs. Whereas M344, SAHA and MS-275 inhibited cell growth at micromolar concentrations, VPA was efficient in a millimolar concentration range (Fig. 1). Logistic curve fitting revealed all curve slopes to be larger than unity (F-test, $P < 0.05$) amounting to $n_{H,MS\text{-}275} = 1.95 \pm 0.33$; $n_{H,SAHA} = 1.52 \pm 0.15$, $n_{H,VPA} = 1.75 \pm 0.21$, $n_{H,M344} = 1.78 \pm 0.31$ (Fig. 1). Equieffective IC_{90} concentrations (defined as concentration causing a 90% reduction of cell viability) were calculated as following: VPA = 4.5 mM, SAHA = 4.9 µM, M344 = 2.9 µM and MS-275 = 12.9 µM. As demonstrated in previous studies, increased levels of the cell cycle control protein $p21^{WAF1}$ were observed in neoplastic cells after HDAC inhibitor treatment [9, 17, 30]. Increased $p21^{WAF1}$ levels were confirmed in B16/F10 melanoma cells after HDAC inhibitor treatment (Fig. 2a). However, compared to the other HDAC inhibitors used in this study (at equieffective IC_{90} concentrations, see above), only MS-275 showed a prominent up-regulation of $p21^{WAF1}$ at 24 h.

The capacity of MS-275 and SAHA to inhibit HDAC activity was identified by immunoblotting of acetylated histone H3 (Fig. 2b). Treatment of B16/F10 cells with IC_{90} doses of MS-275 and SAHA for 24 h caused a prominent increase of acetylated histone H3 protein. Flow cytometry of B16/F10 melanoma cells incubated with MS-275 (IC_{90}) and SAHA (IC_{90}) revealed a significant G1 cell cycle arrest after 24 h (Fig. 3a, b) as well as after 48 and 72 h. The content of tumor cells accumulating

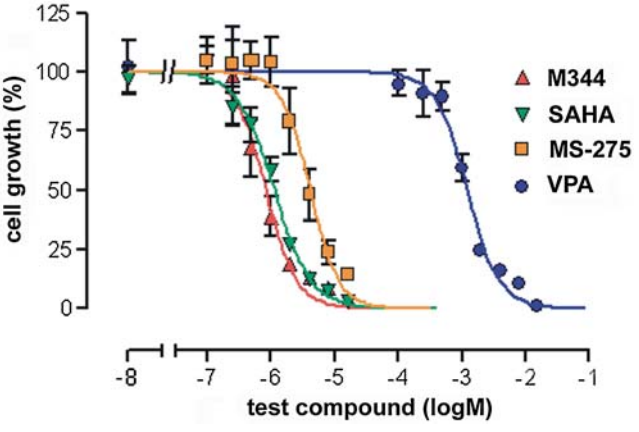

Fig. 1 Proliferation assay of malignant melanoma monolayer B16/F10 cell cultures. MTT assay. *Ordinate*: cell viability as a percentage of the control value in the absence of histone deacetylase (HDAC) inhibitors. *Abscissa*: log concentration of the tested compounds. Inhibitory concentration (IC) of the tested compounds were read from the best-fit curves inducing an inhibition of cell viability to 50 or 90% of the control value and given as pIC_{50} and pIC_{90} values, respectively. All curve slopes were larger than unity (F-test, $P > 0.05$). Therefore, the pIC_{50} and pIC_{90} values were obtained from curves with variable curve slopes. IC values amounted to: $IC_{50,SAHA}$ 1.15 µM; $IC_{90,SAHA}$ 4.9 µM; $IC_{50,VPA}$ 1.26 mM; $IC_{90,VPA}$ 4.47 mM; $IC_{50,M344}$ 0.89 µM; $IC_{90,M344}$ 2.88 µM, $IC_{50,MS\text{-}275}$ 1.48 µM; $IC_{90,MS\text{-}275}$ 12.9 µM. The melanoma cells were treated with respective HDAC inhibitors for 96 h

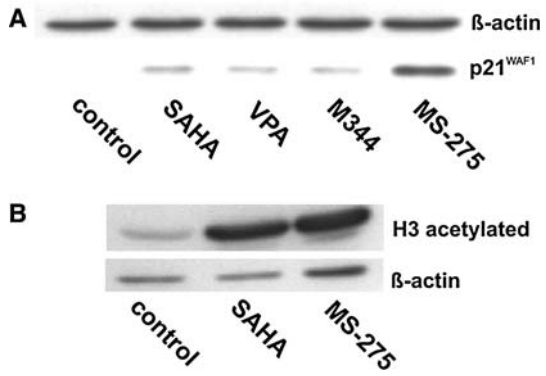

Fig. 2 Immunoblotting of $p21^{WAF1}$ and histone H3 after histone deacetylase (HDAC) inhibitor treatment. **a** Treatment of B16/F10 melanoma cells with IC_{90} concentrations of M344, suberoylanilide hydroxamic acid (SAHA), VPA and MS-275 for 24 h induced up-regulation of the cell cycle inhibitor protein $p21^{WAF1}$ compared to naive controls. **b** HDAC inhibitory effect induced by IC_{90} concentrations of MS-275 and SAHA was verified by histone H3 acetylation status of B16/F10 cells. β-Actin was used as control for equal protein loading

in the sub-G1 phase, which included apoptotic DNA fragmentation, increased from 12% (24 h after IC_{90} treatment) to 42% (72 h after IC_{90} treatment; Fig. 3a). SAHA and MS-275 had similar effects on DNA fragmentation after 72 h (Fig. 3c).

Histone deacetylase inhibitors reduce murine melanoma progression in the organotypic brain metastasis model

We employed rodent hippocampal slice cultures to monitor melanoma proliferation and brain invasion within the organotypic environment [10]. The eGFP-labeled B16/F10 melanoma cells were implanted into the entorhinal cortex (Fig. 4). Continuous tumor growth was observed in untreated control experiments at all time periods (Figs. 4, 7, 8). Histopathological analysis confirmed pigment-laden tumor cells to invade the organotypic rat brain tissue (Fig. 4c, d). Eight days after implantation, this increase amounted up to 228% (Fig. 7a) compared to the initial tumor size 1 day after implantation (defined as 100%). HDAC inhibitors were added to the slice medium, penetrated tissue and exhibited their action on infiltrating tumor cells. As observed in monolayer cell culture (Fig. 2a), tumor cells transplanted into slice cultures were immunopositive for $p21^{WAF1}$ 24 h after MS-275 (Fig. 5a) and SAHA (Fig. 5c) treatment. Untreated controls showed little or no immunoreactivity (Fig. 5d). $p21^{WAF1}$ expression decreased when MS-275 treatment periods were extended to 48 h (Fig. 5b). Treatment of organotypic rat brain slices was performed with equieffective concentrations of SAHA and MS-275 (IC_{90}, twofold IC_{90} or threefold IC_{90}; see above) 1 day after melanoma cell transplantation and every second day thereafter. MS-275 showed a significant

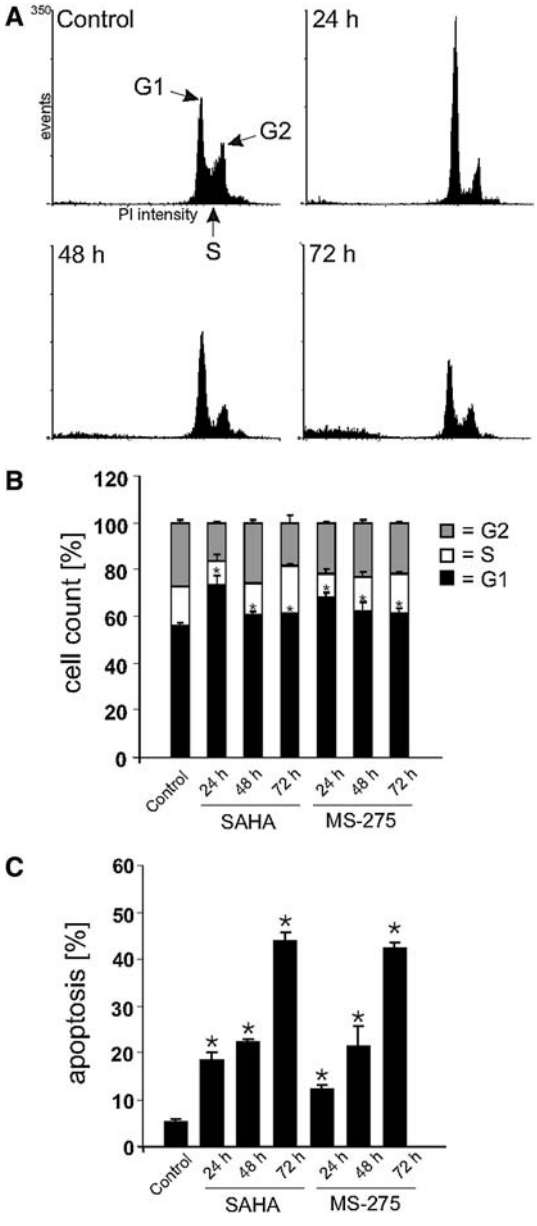

Fig. 3 MS-275 and suberoylanilide hydroxamic acid (SAHA) induce cell cycle arrest and apoptosis. **a** MS-275 (IC_{90}) exposition of B16/F10 cells induced a significant G1 arrest after 24, 48 and 72 h compared to controls. The content of G1 phase cells decreased with exposure time, while the amount of sub-G1 fraction events increased during this time interval. Cells were stained after MS-275 treatment with propidium iodide (PI). The incorporated PI content was measured from a total amount of 10,000 events by FACS analysis. The first peak is defined as G1 cell population and the sub-G1 content as apoptosis. **a** Scale for *abscissa* and *ordinate* given in *upper left image* (control) applies also to other graphs of this panel. **b** Growth phase (G1/S/G2) assignment of cell content after sub-G1 fraction exclusion. Cells were treated with SAHA (IC_{90}) and MS-275 (IC_{90}) for various time periods. In all measurements, increased G1 levels reached significance compared to controls. **c** Quantity of sub-G1 fraction events (apoptosis rate) according to treatment period is increasing. Each measurement was repeated three times and statistical analysis in relation to control was evaluated by Mann–Whitney *U* test. *Asterisks* indicate statistical significance ($P < 0.05$)

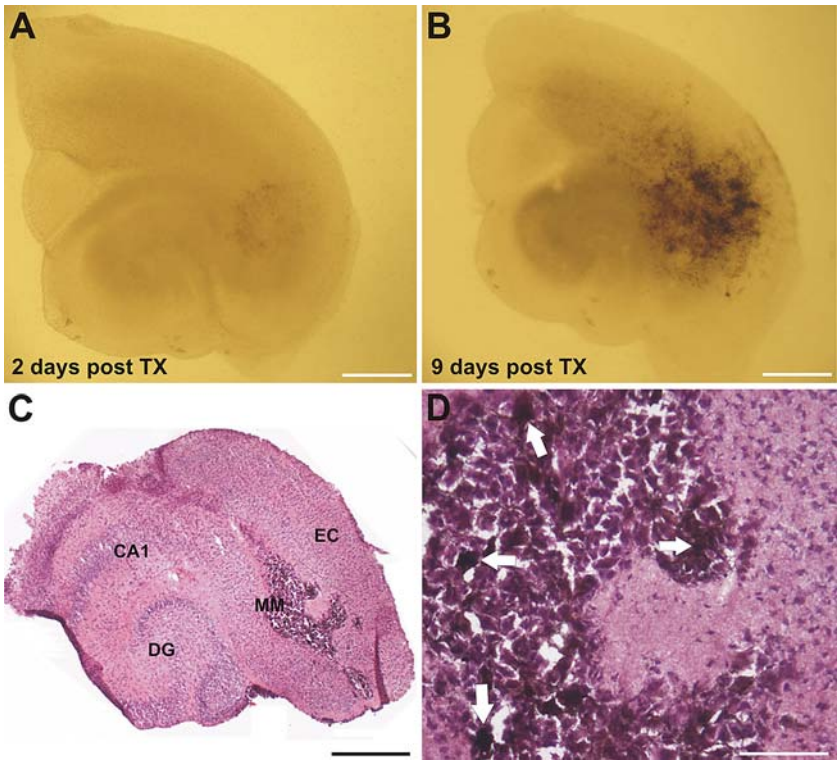

Fig. 4 Ex vivo model of melanomas transplanted into organotypic brain slice cultures. eGFP transfected B16/F10 melanoma cells were implanted into the entorhinal cortex 1 day after slice preparation. Two days later, slight pigmentation of tumor cells could be observed (**a**), whereas 9 days after implantation (**b**) tumor size judged by melanin pigment load expanded dramatically. Beside radial growth, melanomas also invade into the hippocampal formation (**c**). Cryosections of slices stained with hematoxylin–eosin confirmed tumor invasion into the organotypic slice culture (**c**). **d** A magnified view of the tumor transplant revealed melanoma cells heavily laden with melanin pigment (*white arrows*). Abbreviations in **c**: *CA1* Cornu amonis 1, *DG* dentate gyrus, *EC* entorhinal cortex, *MM* malignant melanoma. Scale bar encoded in **a** and **b** = 1 mm, in **c** = 500 μm and in **d** = 100 μm

reduction of tumor growth as measured by fluorescence microscopy (Figs. 6a, c, d, 7a). Dose escalation experiments using two- and threefold IC_{90} of MS-275 revealed progressive tumor reduction compared to time matched controls (Fig. 7). In contrast to MS-275, a threefold IC_{90} dosage escalation of SAHA was less effective to diminish tumor growth in the rat organotypic slice culture environment (Fig. 6e). These data were confirmed in an allogenic murine transplantation model (Fig. 7b) using the same conditions as described before. However, transplanted melanoma cells tended to grow more rapidly (359% at 6 DaT) in untreated murine brain tissue (Fig. 7b) than in rat slices (217% at 6 DaT; Fig. 7a). Moreover, a twofold IC_{90} dosage of MS-275 was sufficient to inhibit melanoma growth comparable to the threefold dosage used in rat slice cultures, whereas no differences were observed between rat and mouse cultures using SAHA (Fig. 7). Similar results were obtained after 6 days of HDAC inhibitor treatment of a firmly established tumor, i.e., treatment started 4 days after tumor transplantation (Fig. 8).

Histopathological analysis of slice cultures treated with MS-275 confirmed cell death in the majority of malignant melanoma cells (Fig. 6b). Pyknotic cell nuclei as well as extracellular pigment deposits within the transplanted tumor site were thus considered as histopathological hallmarks of the ex vivo MS-275 therapy.

Histone deacetylase inhibitors reduce human melanoma growth in vitro and ex vivo

Additional experiments were performed using primary human melanoma cell lines MM1 and MM2 obtained from surgically removed melanoma metastasis [38]. All tested HDAC inhibitors were able to reduce cell growth in vitro with the exception of VPA, at micromolar concentrations (MTT assay, Fig. 9a). All compounds induced the cell cycle inhibitor p21 concentration-dependently (data not shown). Moreover, FACS analysis revealed prominent induction of apoptosis after 48–72 h of treatment with SAHA and MS-275 (Fig. 9b). Finally, MM2 cells were transplanted into rat organotypic hippocampal slice cultures. These cells were treated 24 h after transplantation with either SAHA (IC_{90}) or MS-275 (IC_{90}). Compared to untreated controls and SAHA treated experiments, MS-275 significantly reduced tumor size (Fig. 9c). Transplantation of MM1 cells yielded similar results (data not shown).

Discussion

Tumor cell transplantation into organotypic slice cultures of murine and rat hippocampus were employed to model brain metastases of malignant melanomas. Within this experimental ex vivo model, we identified the benzamide MS-275 as a promising anti-cancer drug for chemotherapy strategies. In a first approach, B16/F10 melanoma cells have been targeted by the HDAC inhibiting action of short-chain fatty acids (VPA), hydroxamic acids (SAHA), as well as benzamides (MS-275 and M344), which resulted in decreased cell proliferation in vitro. Our further analyses focused, however, on SAHA and MS-275 since VPA was effective only at millimolar concentrations (Fig. 1) not likely to be achieved in clinical

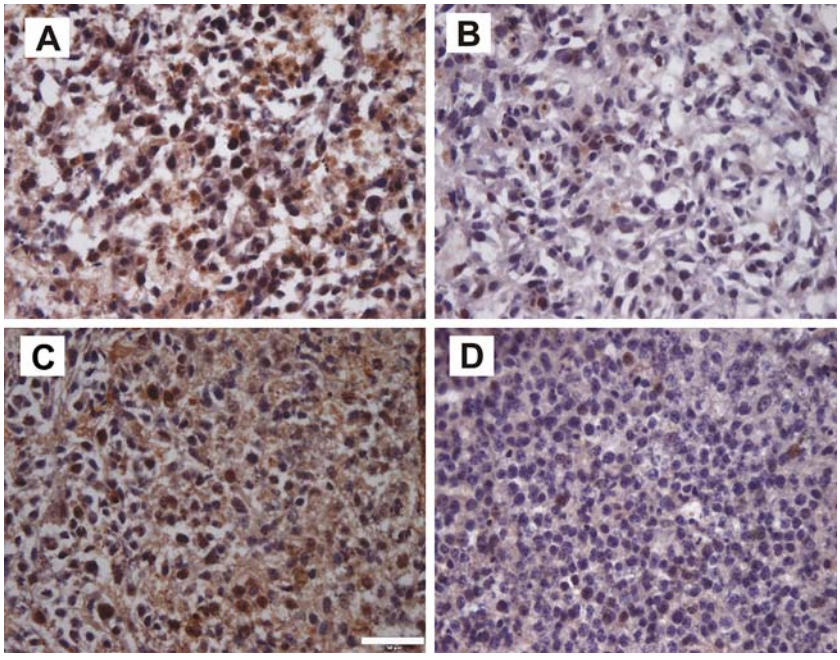

Fig. 5 MS-275 increase $p21^{WAF1}$ expression in melanoma cells transplanted into organotypic slice cultures. Increased p21 expression in B16/F10 melanoma cells transplanted onto hippocampal murine slices following inhibitors of histone deacetylases treatment. **a** MS-275 ($1 \times IC_{90}$) for 24 h. **c** Suberoylanilide hydroxamic acid ($3 \times IC_{90}$) for 24 h. **b** MS-275 ($1 \times IC_{90}$) for 48 h. Untreated tumor cells implanted onto slices were used as control (**d**). Frozen sections were prepared from paraformaldehyde fixed slices and immunostained with antibodies directed against the cell cycle inhibitor p21 with the DAB method. Scale bar = 50 μm

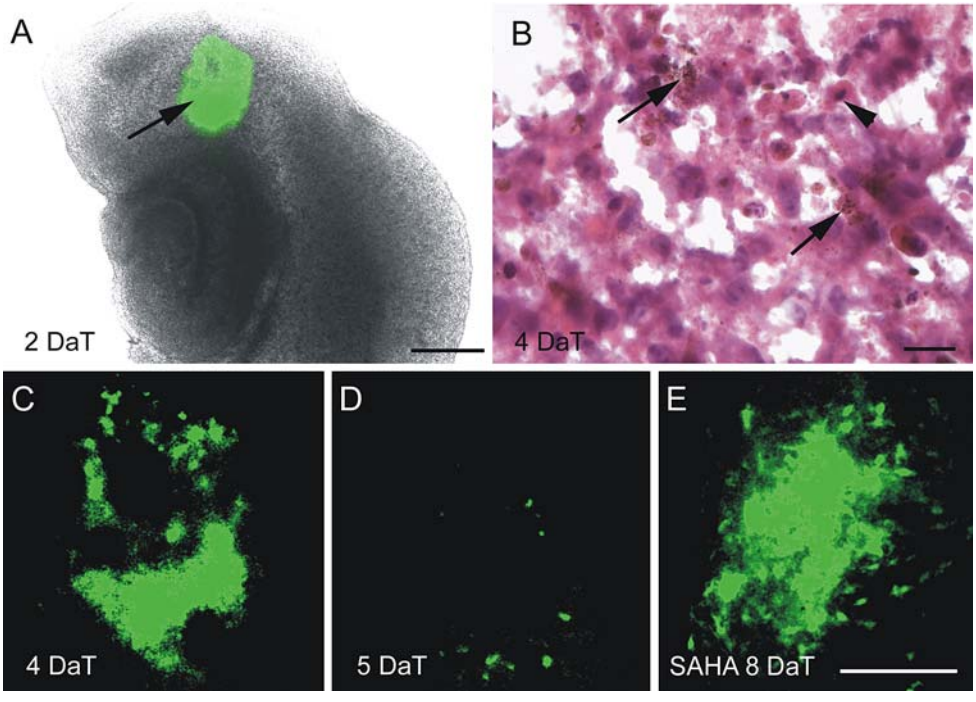

Fig. 6 MS-275 treatment of B16/F10 melanoma cells implanted into organotypic brain slices. Organotypic hippocampal slices transplanted with green fluorescent melanoma cells into the entorhinal cortex (*arrow* in **a**) were treated with MS-275 ($3 \times IC_{90}$) and suberoylanilide hydroxamic acid (SAHA) ($3 \times IC_{90}$). A MS-275 treatment period of 4 days (DaT) induced significant reduction of melanoma cell mass (**c**, **d**). At 5 DaT (**d**) only few tumor cells remain detectable by fluorescence microscopy, whereas 8 DaT virtually no fluorescence signal could be detected (data not shown). Histopathological analysis confirmed tumor cell death following MS-275 treatment (**b**). *Arrows* in **b** point to extracellular pigment deposits detected in a 12 μm thin hematoxylin–eosin stained section. *Arrowhead* indicates a pyknotic nucleus, compatible with irreversible cell damage. **e** In contrast to ex vivo MS-275 treatment, a fluorescent tumor mass remains visible 8 DaT following SAHA administration. Scale bar encoded in **a** = 1 mm, in **b** = 20 μm and in **e** (applies also to **c** and **d**) = 500 μm

trials. In addition, M344 is not yet been fully characterized with respect to passing the blood–brain barrier. As probable molecular anti-cancer mechanism, MS-275 and SAHA transiently up-regulate $p21^{WAF1}$ gene expression in a p53-independent manner (Figs. 2, 5) [17, 50]. High intracellular levels of $p21^{WAF1}$ arrest the cell cycle at

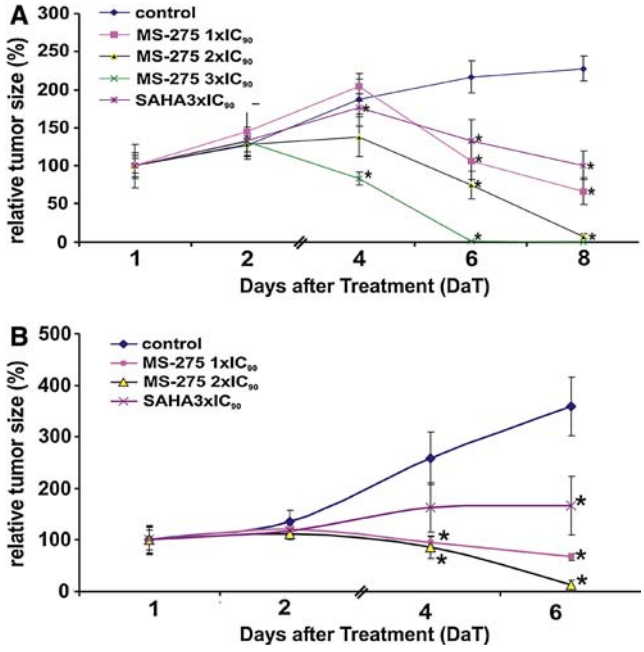

Fig. 7 Tumor growth in rodent hippocampal slice cultures. **a** Monitoring of B16/F10 tumor cell growth in rat organotypic slice cultures using fluorescent microscopy. Note that inhibition of tumor growth correlated with dosage escalation for MS-275. Each experiment was repeated seven times and statistical analysis in relation to control was evaluated by Mann–Whitney *U* test. *Asterisks* indicate statistical significance compared to control levels ($P < 0.05$). **b** Organotypic mouse hippocampal slices containing transplanted green fluorescent B16/F10 melanoma cells were treated with MS-275 ($1 \times IC_{90}$; $2 \times IC_{90}$) and suberoylanilide hydroxamic acid ($3 \times IC_{90}$) for 6 days (DaT). Microscopic monitoring of tumor growth in controls and histone deacetylase inhibitor treated allogeneic slice cultures revealed significant inhibition of tumor growth correlating with dosage escalation. Each experiment was repeated seven times and statistical analysis of tumor growth in relation to control was evaluated by Mann–Whitney *U* test. *Asterisks* indicate statistical significance compared to control levels ($P < 0.05$)

phase G1, which could also be confirmed in our experiments (Fig. 3). HDAC inhibitors target also other molecules which critically control the cell cycle, i.e., p19 [49]. It is unlikely that this mechanism plays a role in our model, as the p19 locus is deleted in the B16/F10 melanoma cell line (data not shown, see also reference [32]). However, it underscores the importance of a given genetic background when facing variable chemotherapeutic efficacies of epigenetic treatment strategies.

In our experimental set-up, the anti-tumor action of MS-275 was superior to SAHA, although both compounds had similar efficacies in monolayer assays. Indeed, the HDAC inhibitory propensity of the benzamide MS-275 is different compared to the hydroxamate SAHA. This is likely to result from their degree of specificity for HDAC enzymes. There are three classes of HDACs comprising a family of 18 protein members [16]. Whereas SAHA inhibits a broader spectrum of HDACs (classes I and II) [31], MS-275 targets mainly class I HDAC1 [13, 22, 28], and at higher concentrations also class II HDAC6 [14, 33]. Accordingly, HDAC1 interacts with the E2F transcription factor and retinoblastoma tumor suppressor protein. This complex is involved in progression of G1 phase by regulating cell cycle relevant protein transcription [3].

Recent data indicate that HDAC inhibitors induce also caspase-dependent apoptotic cell death [5]. The propensity of SAHA or MS-275 to target intrinsic proapoptotic pathways in malignant tumor cells, including melanomas, have been shown in various experimental studies [11, 29, 42]. These data are compatible with the observation that the amount of the "apoptotic" subG1 cell cycle fraction increased with time (Figs. 3c, 9b), whereas the G1 fraction decreased already after 48 and 72 h (Fig. 3b). The latter finding may also relate to transient $p21^{WAF1}$ expression returning to basal levels after 48 h (Fig. 5a, b) [39, 41, 42].

Clinical trials support the beneficial propensity of HDAC inhibitors for the treatment of cancer. MS-275 shows a good bioavailability with little side effects as well as reduction of tumor growth in a preliminary phase I/II trial [34]. Moreover, MS-275 sensitizes tumor cells for radiation therapy [5]. Synergistic effects of these two treatment modalities may increase clinical outcome in

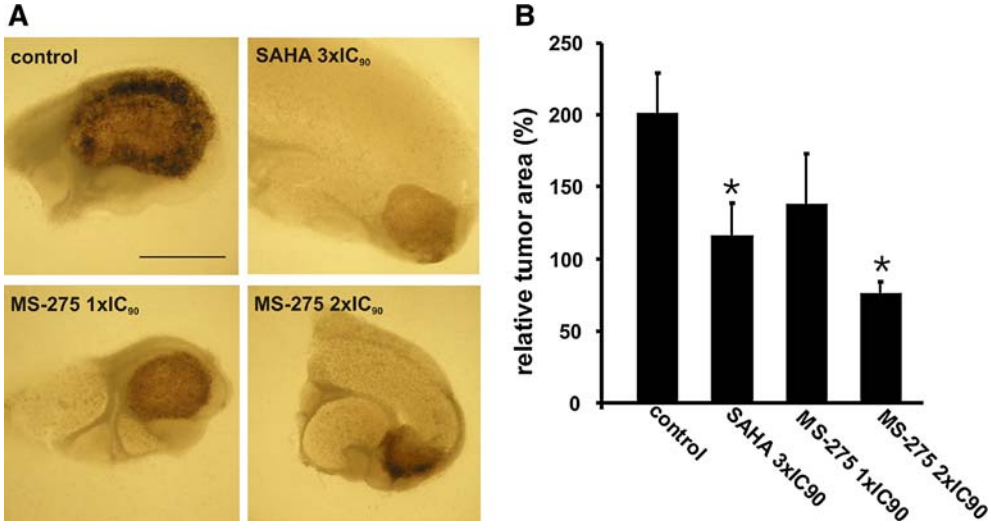

Fig. 8 Histone deacetylase (HDAC) inhibitors reduce murine melanoma growth in established tumors. **a** B16/F10 cells were transplanted onto mouse hippocampal slice cultures 1 day after preparation. HDAC inhibitor treatment was started 4 days later for a period of 6 days. **b** Tumor growth was quantified in relation to controls 6 days after treatment with suberoylanilide hydroxamic acid (threefold IC_{90}), MS-275 (onefold IC_{90} or twofold IC_{90}). Tumor size 4 days after transplantation was set = 100%. All experiments were repeated six times. *Asterisks* mark significant tumor reduction as verified by Mann–Whitney *U* test. Scale bar in **a** = 1 mm

A

IC_{90}	MM1	MM2
SAHA (μM)	3,39	14,1
M344 (μM)	1,51	1,78
MS-275 (μM)	4,57	3,89
VPA (mM)	1,35	0,87

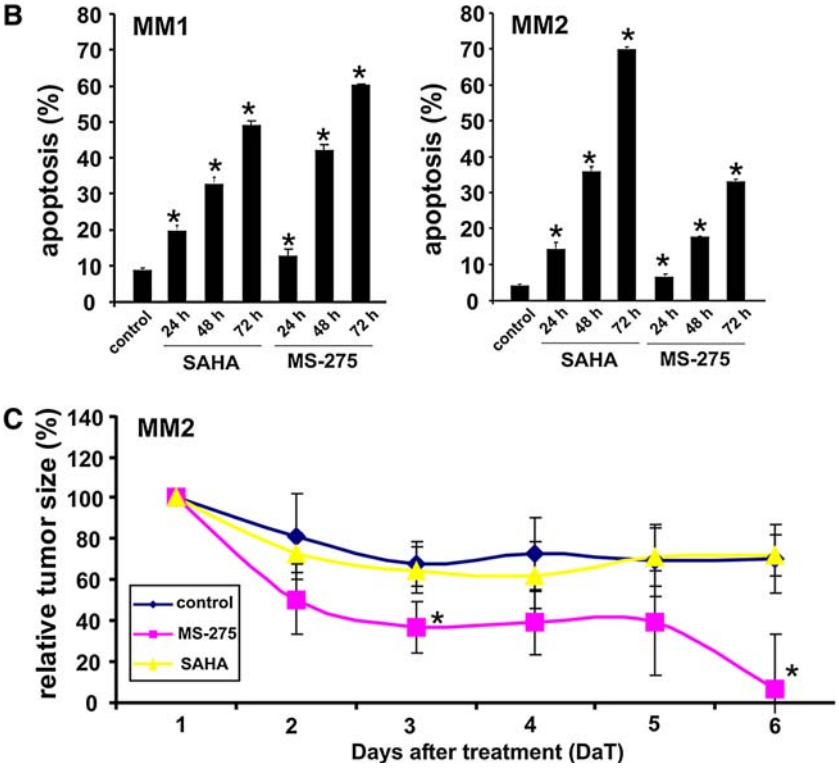

Fig. 9 In vitro and ex vivo validation of histone deacetylase inhibitors in human melanoma cell lines. **a** Concentrations of tested compounds were analyzed in human melanoma cell lies MM1 and MM2 (MTT assay) and given as IC_{90} values. **b** FACS analyses of human melanoma cells revealed a time dependent increase of the apoptotic fraction after treatment with IC_{90} of suberoylanilide hydroxamic acid (SAHA) and MS-275. Experiments were repeated three times. **c** Human melanoma cells (MM2) were transplanted into rat hippocampal slice cultures and treated 1 day thereafter with IC_{90} of SAHA and MS-275 for 6 days. Tumor growth was monitored by fluorescence microscopy. Each experiment was repeated seven times and statistical analysis was evaluated by Mann–Whitney *U* test. *Asterisks* indicate statistical significance (calculated for the end point of experimental time course compared to control levels; $P < 0.05$)

affected patients. MS-275 crosses the blood–brain barrier [44], rendering it a promising drug also in the treatment of brain metastases or other neurological disorders [4, 21]. However, availability of brain tissue for experimental modeling of brain metastases or other neoplastic disorders is restricted. Organotypic slice cultures of rodent brain may bridge this gap. Slice cultures have a defined small volume of 1.2 ml allowing systematic testing of pharmacological compounds. This assay allows to evaluate therapeutic efficacies in a more complex organotypic environment as compared to the restricted monolayer assay. Surprisingly, in our model SAHA failed to achieve similar anti-melanoma potency as MS-275 (Figs. 6, 7, 9). HDAC inhibitors also reduced the size of firmly established tumors (Fig. 8), indicating their chemotherapeutic potential for the treatment of melanoma brain metastasis. These substances also arrested tumor growth of human cell lines in vitro and ex vivo (Fig. 9), further confirming their clinical impact. Moreover, this model may provide a useful tool to address further molecular pathomechanisms of melanoma progression and spreading into the CNS. Melanoma cells grow and invade a nearly authentic brain microenvironment and extracellular matrix which is likely to interact with tumor cell proliferation and apoptosis signaling pathways in a more complex fashion compared to in vitro situations. Notwithstanding, predictions including melanoma cell growth based on perfusion and/or peripheral crosstalk of brain tissue, are restricted in our model and need further confirmation in vivo. Nevertheless, accessible microscopical monitoring of transplanted tumor cells is valuable for a translational approach with respect to dose escalation studies requiring precise estimations of drug concentrations as well as screening amongst a large number of promising new chemotherapeutics.

Acknowledgments We kindly acknowledge Dr P. Rohwer, Nikolaus-Fiebiger-Center of Molecular Medicine, University of Erlangen-Nuremberg for assistance with fluorescence tumor cell sorting. We thank Tajana Jungbauer, Ina Jeske, Silke Gutmann and Birte Rings for technical support.

References

1. Agarwala SS, Kirkwood JM, Gore M, Dreno B, Thatcher N, Czarnetski B, Atkins M, Buzaid A, Skarlos D, Rankin EM

(2004) Temozolomide for the treatment of brain metastases associated with metastatic melanoma: a phase II study. J Clin Oncol 22:2101–2107
2. Bafaloukos D, Gogas H (2004) The treatment of brain metastases in melanoma patients. Cancer Treat Rev 30:515–520
3. Brehm A, Miska EA, McCance DJ, Reid JL, Bannister AJ, Kouzarides T (1998) Retinoblastoma protein recruits histone deacetylase to repress transcription. Nature 391:597–601
4. Brichta L, Hofmann Y, Hahnen E, Siebzehnrubl FA, Raschke H, Blumcke I, Eyüpoglu IY, Wirth B (2003) Valproic acid increases the SMN2 protein level: a well-known drug as a potential therapy for spinal muscular atrophy. Hum Mol Genet 12:2481–2489
5. Burgess A, Ruefli A, Beamish H, Warrener R, Saunders N, Johnstone R, Gabrielli B (2004) Histone deacetylase inhibitors specifically kill nonproliferating tumour cells. Oncogene 23:6693–6701
6. Camphausen K, Scott T, Sproull M, Tofilon PJ (2004) Enhancement of xenograft tumor radiosensitivity by the histone deacetylase inhibitor MS-275 and correlation with histone hyperacetylation. Clin Cancer Res 10:6066–6071
7. Eyüpoglu I, Hahnen E, Tränkle C, Savaskan NE, Siebzehnrubl F, Buslei R, Lemke D, Wick W, Fahlbusch R, Blumcke I (2006) Experimental therapy of malignant gliomas using the inhibitor of histone deacetylases MS-275. Mol Cancer Ther 5:1248–1255
8. Eyüpoglu IY, Bechmann I, Nitsch R (2003) Modification of microglia function protects from lesion-induced neuronal alterations and promotes sprouting in the hippocampus. FASEB J 17:1110–1111
9. Eyüpoglu IY, Hahnen E, Buslei R, Siebzehnrubl FA, Savaskan NE, Luders M, Trankle C, Wick W, Weller M, Fahlbusch R, Blumcke I (2005a) Suberoylanilide hydroxamic acid (SAHA) has potent anti-glioma properties in vitro, ex vivo and in vivo. J Neurochem 93:992–999
10. Eyüpoglu IY, Hahnen E, Heckel A, Siebzehnrubl FA, Buslei R, Fahlbusch R, Blumcke I (2005b) Malignant glioma-induced neuronal cell death in an organotypic glioma invasion model. J Neurosurg 102:738–744
11. Facchetti F, Previdi S, Ballarini M, Minucci S, Perego P, La Porta CA (2004) Modulation of pro- and anti-apoptotic factors in human melanoma cells exposed to histone deacetylase inhibitors. Apoptosis 9:573–582
12. Fife KM, Colman MH, Stevens GN, Firth IC, Moon D, Shannon KF, Harman R, Petersen-Schaefer K, Zacest AC, Besser M, Milton GW, McCarthy WH, Thompson JF (2004) Determinants of outcome in melanoma patients with cerebral metastases. J Clin Oncol 22:1293–1300
13. Fournel M, Trachy-Bourget MC, Yan PT, Kalita A, Bonfils C, Beaulieu C, Frechette S, Leit S, Abou-Khalil E, Woo SH, Delorme D, MacLeod AR, Besterman JM, Li Z (2002) Sulfonamide anilides, a novel class of histone deacetylase inhibitors, are antiproliferative against human tumors. Cancer Res 62:4325–4330
14. Furumai R, Komatsu Y, Nishino N, Khochbin S, Yoshida M, Horinouchi S (2001) Potent histone deacetylase inhibitors built from trichostatin A and cyclic tetrapeptide antibiotics including trapoxin. Proc Natl Acad Sci USA 98:87–92
15. Glaser KB, Staver MJ, Waring JF, Stender J, Ulrich RG, Davidsen SK (2003) Gene expression profiling of multiple histone deacetylase (HDAC) inhibitors: defining a common gene set produced by HDAC inhibition in T24 and MDA carcinoma cell lines. Mol Cancer Ther 2:151–163
16. Glozak MA, Sengupta N, Zhang X, Seto E (2005) Acetylation and deacetylation of non-histone proteins. Gene 363:15–23
17. Gui CY, Ngo L, Xu WS, Richon VM, Marks PA (2004) Histone deacetylase (HDAC) inhibitor activation of p21WAF1 involves changes in promoter-associated proteins, including HDAC1. Proc Natl Acad Sci USA 101:1241–1246
18. Hallberg O, Johansson O (2004) Malignant melanoma of the skin—not a sunshine story! Med Sci Monit 10:CR336–CR340
19. Helmbach H, Rossmann E, Kern MA, Schadendorf D (2001) Drug-resistance in human melanoma. Int J Cancer 93:617–622
20. Hersey P, Menzies SW, Coventry B, Nguyen T, Farrelly M, Collins S, Hirst D, Johnson H (2005) Phase I/II study of immunotherapy with T-cell peptide epitopes in patients with stage IV melanoma. Cancer Immunol Immunother 54:208–218
21. Hockly E, Richon VM, Woodman B, Smith DL, Zhou X, Rosa E, Sathasivam K, Ghazi-Noori S, Mahal A, Lowden PA, Steffan JS, Marsh JL, Thompson LM, Lewis CM, Marks PA, Bates GP (2003) Suberoylanilide hydroxamic acid, a histone deacetylase inhibitor, ameliorates motor deficits in a mouse model of Huntington's disease. Proc Natl Acad Sci USA 100:2041–2046
22. Hu E, Dul E, Sung CM, Chen Z, Kirkpatrick R, Zhang GF, Johanson K, Liu R, Lago A, Hofmann G, Macarron R, de los Frailes M, Perez P, Krawiec J, Winkler J, Jaye M (2003) Identification of novel isoform-selective inhibitors within class I histone deacetylases. J Pharmacol Exp Ther 307:720–728
23. Huuskonen J, Suuronen T, Miettinen R, van Groen T, Salminen A (2005) A refined in vitro model to study inflammatory responses in organotypic membrane culture of postnatal rat hippocampal slices. J Neuroinflammation 2:25
24. Jenuwein T, Allis CD (2001) Translating the histone code. Science 293:1074–1080
25. Jung M, Brosch G, Kolle D, Scherf H, Gerhauser C, Loidl P (1999) Amide analogues of trichostatin A as inhibitors of histone deacetylase and inducers of terminal cell differentiation. J Med Chem 42:4669–4679
26. Khayat D, Giroux B, Berille J, Cour V, Gerard B, Sarkany M, Bertrand P, Bizzari JP (1994) Fotemustine in the treatment of brain primary tumors and metastases. Cancer Invest 12:414–420
27. Krishan A (1975) Rapid flow cytofluorometric analysis of mammalian cell cycle by propidium iodide staining. J Cell Biol 66:188–193
28. Li J, Staver MJ, Curtin ML, Holms JH, Frey RR, Edalji R, Smith R, Michaelides MR, Davidsen SK, Glaser KB (2004) Expression and functional characterization of recombinant human HDAC1 and HDAC3. Life Sci 74:2693–2705
29. Lucas DM, Davis ME, Parthun MR, Mone AP, Kitada S, Cunningham KD, Flax EL, Wickham J, Reed JC, Byrd JC, Grever MR (2004) The histone deacetylase inhibitor MS-275 induces caspase-dependent apoptosis in B-cell chronic lymphocytic leukemia cells. Leukemia 18:1207–1214
30. Marks PA (2004) The mechanism of the anti-tumor activity of the histone deacetylase inhibitor, suberoylanilide hydroxamic acid (SAHA). Cell Cycle 3:534–535
31. Marks PA, Richon VM, Miller T, Kelly WK (2004) Histone deacetylase inhibitors. Adv Cancer Res 91:137–168
32. Melnikova VO, Bolshakov SV, Walker C, Ananthaswamy HN (2004) Genomic alterations in spontaneous and carcinogen-induced murine melanoma cell lines. Oncogene 23:2347–2356
33. Miller TA, Witter DJ, Belvedere S (2003) Histone deacetylase inhibitors. J Med Chem 46:5097–5116
34. Monneret C (2005) Histone deacetylase inhibitors. Eur J Med Chem 40:1–13
35. Mosmann T (1983) Rapid colorimetric assay for cellular growth and survival: application to proliferation and cytotoxicity assays. J Immunol Methods 65:55–63
36. Murakami T, Cardones AR, Hwang ST (2004) Chemokine receptors and melanoma metastasis. J Dermatol Sci 36:71–78
37. Nakamura K, Yoshikawa N, Yamaguchi Y, Kagota S, Shinozuka K, Kunitomo M (2002) Characterization of mouse melanoma cell lines by their mortal malignancy using an experimental metastatic model. Life Sci 70:791–798
38. Nettelbeck DM, Rivera AA, Davydova J, Dieckmann D, Yamamoto M, Curiel DT (2003) Cyclooxygenase-2 promoter for tumour-specific targeting of adenoviral vectors to melanoma. Melanoma Res 13:287–292
39. Park JH, Jung Y, Kim TY, Kim SG, Jong HS, Lee JW, Kim DK, Lee JS, Kim NK, Bang YJ (2004) Class I histone deacetylase-selective novel synthetic inhibitors potently inhibit human tumor proliferation. Clin Cancer Res 10:5271–5281
40. Radbill AE, Fiveash JF, Falkenberg ET, Guthrie BL, Young PE, Meleth S, Markert JM (2004) Initial treatment of melanoma

brain metastases using gamma knife radiosurgery: an evaluation of efficacy and toxicity. Cancer 101:825–833
41. Richon VM, Sandhoff TW, Rifkind RA, Marks PA (2000) Histone deacetylase inhibitor selectively induces p21WAF1 expression and gene-associated histone acetylation. Proc Natl Acad Sci USA 97:10014–10019
42. Rosato RR, Almenara JA, Grant S (2003) The histone deacetylase inhibitor MS-275 promotes differentiation or apoptosis in human leukemia cells through a process regulated by generation of reactive oxygen species and induction of p21CIP1/WAF1 1. Cancer Res 63:3637–3645
43. Sambrook J, Russell DW (2001) Molecular cloning. In: Introducing cloned genes into cultured mammalian cells. CSHL Press, Cold Spring Harbour
44. Simonini MV, Camargo LM, Dong E, Maloku E, Veldic M, Costa E, Guidotti A (2006) The benzamide MS-275 is a potent, long-lasting brain region-selective inhibitor of histone deacetylases. Proc Natl Acad Sci USA 103:1587–1592
45. Stein TD, Anders NJ, DeCarli C, Chan SL, Mattson MP, Johnson JA (2004) Neutralization of transthyretin reverses the neuroprotective effects of secreted amyloid precursor protein (APP) in APPSW mice resulting in tau phosphorylation and loss of hippocampal neurons: support for the amyloid hypothesis. J Neurosci 24:7707–7717
46. Stoppini L, Buchs PA, Muller D (1991) A simple method for organotypic cultures of nervous tissue. J Neurosci Methods 37:173–182
47. de Vries E, Coebergh JW (2004) Cutaneous malignant melanoma in Europe. Eur J Cancer 40:2355–2366
48. Wisinski KB (2003) A phase I study of an oral histone deacetylase inhibitor, MS-275 in patients with refractory solid tumors and lymphomas. Proc Am Soc Clin Oncol 22:802
49. Yokota T, Matsuzaki Y, Miyazawa K, Zindy F, Roussel MF, Sakai T (2004) Histone deacetylase inhibitors activate INK4d gene through Sp1 site in its promoter. Oncogene 23:5340–5349
50. Yoshida M, Furumai R, Nishiyama M, Komatsu Y, Nishino N, Horinouchi S (2001) Histone deacetylase as a new target for cancer chemotherapy. Cancer Chemother Pharmacol 48(Suppl. 1):S20–S26